



## Research Article

<https://doi.org/10.1631/jzus.B2300617>



# Co-culture of natural killer cells and tumor spheroids on a heterogeneous multilayer paper stack

Yuanyuan XIE<sup>1</sup>, Xiaoyan YANG<sup>1</sup>, Rong PAN<sup>1</sup>, Lixia GAO<sup>2</sup>, Ling YU<sup>1</sup>✉

<sup>1</sup>Key Laboratory of Luminescence Analysis and Molecular Sensing, Ministry of Education, Institute for Clean Energy and Advanced Materials, School of Materials and Energy, Southwest University, Chongqing 400715, China

<sup>2</sup>National & Local Joint Engineering Research Center of Targeted and Innovative Therapeutics, College of Pharmacy & International Academy of Targeted Therapeutics and Innovation, Chongqing University of Arts and Sciences, Chongqing 402160, China

**Abstract:** Multilayer paper-based cell culture, as an *in vitro* three-dimensional (3D) cell culture method, has been frequently used to research drug bioavailability, therapeutic efficacy, and dose-limiting toxicity in malignant tumors. This paper proposes a heterogeneous multilayer paper stacking co-culture system to establish a model of natural killer (NK) cells moving through the endothelium layer and attacking tumor spheroids. This system consists of three layers: a bottom tumor-spheroid layer, a middle invasion layer, and a top endothelium layer. NK-92 cells were placed in the supernatant on top of the three layers. After two days of co-culture, the attack of tumor spheroids by NK cells was observed. We additionally examined the infiltration of NK-92 cells within the tumor spheroids at different Z-axis depths using a confocal microscope, and the results suggested that the system successfully realizes NK cells traveling cross the endothelium layer to form tumor-infiltrating NK cells (TINKs). The potential application of multilayer paper for co-culture models involving cancer cells and immune cells holds great promise for exploring the interaction dynamics of these two cell types.

**Key words:** Multilayer paper stack; Co-culture; Tumor spheroid; Human umbilical vein endothelial cell (HUVEC); Natural killer cell (NK cell); Migration

## 1 Introduction

Prostate cancer is a frequent malignancy that poses a considerable health burden (Łuczyńska and Anioł, 2013). Consequently, intensive research on effective therapies has produced recent advancements in three-dimensional (3D) cell culture, allowing for in-depth investigations into drug bioavailability, therapeutic efficacy, and toxicity regarding malignant tumors (Fontana et al., 2020). Three-dimensional cultures enable cells to retain their morphological and phenotypic characteristics observed *in vivo*, making them invaluable for studying complex cellular behaviors and interactions (Gaitán-Salvatella et al., 2021). To further advance the development of *in vitro* 3D cell culture, several methods have been devised, including

suspension culture (Pan et al., 2023b), concave micro-well culture (Guo et al., 2022), scaffold-based culture (Lin et al., 2021), hanging drop culture (Fu et al., 2021), 3D bioprinting technique (Zhao et al., 2022), and the layer-by-layer cell-coating technique (Choi et al., 2020).

Scaffold-based culture in particular has been widely employed to investigate cell–cell and cell–extracellular matrix (ECM) interactions (Sang et al., 2022). The fibrous structure of paper as scaffold material has been proven effective for 3D cultures due to its ability to support cell migration and the creation of complex *in vitro* microenvironments (Larson et al., 2021). Additionally, the structural characteristics of paper organized into a stacked system facilitate cell migration. The advantages of the multilayer paper cell co-culture system include: (1) the establishment of a 3D complex *in vitro* microenvironment through the multilayer structure; (2) the ability to replicate various cell behaviors, such as cell–cell interactions, cell–ECM interactions, cell invasion, and cell migration; (3) the

✉ Ling YU, [lingyu12@swu.edu.cn](mailto:lingyu12@swu.edu.cn)

Ling YU, <https://orcid.org/0000-0002-6726-281X>

Received Sept. 3, 2023; Revision accepted Mar. 4, 2024;  
Crosschecked Dec. 4, 2024

© Zhejiang University Press 2024

confinement of nutrition, oxygen, and signal molecules to form diffusion gradients (Romo-Herrera et al., 2021); and (4) the ability to investigate cells in each layer of the multilayer paper co-culture system by de-stacking the paper, allowing for simple cell recovery. Despite the recent research focus on scaffold-based methods for modeling tumor–endothelial tissue and tumor–normal tissue interactions, there has been little emphasis on tumor–immune cell models. Hence, the establishment of a multilayer paper-based co-culture system to investigate the interactions between tumor spheroids and endothelial and immune cells is of great significance.

Natural killer (NK) cells, as crucial effector lymphocytes in the peripheral blood, play a critical role in the innate immune system (de Andrade et al., 2019). *In vivo*, a subset of NK cells facilitates tumor-infiltrating NK cells (TINKs) by traveling through the blood vessel wall to enter the tumor tissue (Burster et al., 2021). Traditional studies on tumor–NK interactions have relied on animal models or simplistic *in vitro* co-culture plates, which cannot capture the complexity of the tumor microenvironment and the dynamic nature of cell migration (Varudkar et al., 2021). In contrast, an *in vitro* 3D co-culture system enables the migration of tumor cells and NK cells, as well as the formation of TINKs.

Agar, well known for its cell-repelling properties, supports the formation of tumor spheroids in a microwell plate and on paper scaffold (Pan et al., 2023a). Matrigel, another type of gel derived from Engelbreth-Holm-Swarm mouse tumor cultures, is widely used for organoid cultivation, promoting cell migration and facilitating 3D cell culture (Wu et al., 2023). In addition, the interiors of solidified agar and Matrigel allow nutrition diffusion, such as glucose and amino acid, as well as oxygen transport for cell growth (Agarwal et al., 2020). Thus, agar and Matrigel could be used to functionalize the cellulose scaffold of paper for cell culture.

The objective of this study was to establish a multilayer paper co-culture system for investigating tumor spheroids–human umbilical vein endothelial cell (HUVEC)–NK cell interactions and migration. The co-culture system comprises three distinct layers: the bottom layer features agar-coated paper for tumor spheroid formation; the middle layer is made from Matrigel-coated paper to facilitate cell migration and invasion; and the top layer, also Matrigel-coated,

supports HUVEC growth (Fig. 1a). NK cells are introduced above the top layer, allowing for the tracking of their migration towards the tumor spheroids below. First, the morphology and mechanical properties of the multilayer paper were characterized. Subsequently, the cell behaviors on each layer were investigated. Finally, the movement of NK cells from the top HUVEC layer through the middle Matrigel layer to the bottom tumor spheroid layer was quantified.

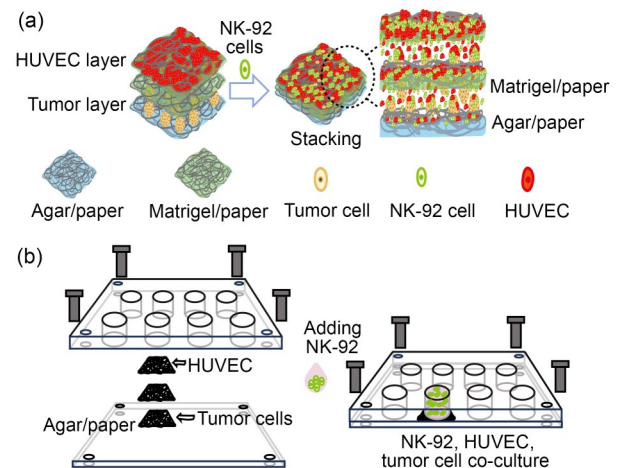


**Fig. 1** Schematic illustration of cell co-culture in the multilayer paper. (a) Cells on the stacked multilayer paper. (b) Assembly of the multilayer paper-based device for cell co-culture. NK: natural killer; HUVEC: human umbilical vein endothelial cell.

## 2 Materials and methods

### 2.1 Materials and reagents

Human prostate cancer cells (DU145), human prostate epithelial cells (PNT1A), and HUVECs were obtained from the cell bank of the Chinese Academy of Sciences (Shanghai, China). Human NK-92 cells were from Procell (Wuhan, China). The DU145, PNT1A, and HUVECs were maintained in Dulbecco's modified Eagle's medium (DMEM; Gibco, USA), containing fetal bovine serum (10% (volume fraction), Bio-Channel, Nanjing, China), penicillin (100 U/mL), and streptomycin (100  $\mu$ g/mL) at 37  $^{\circ}$ C in a 5%  $\text{CO}_2$  atmosphere. The NK-92 cells were maintained in NK-92 special medium (Cat# CM-0530, Procell, Wuhan, China), also at 37  $^{\circ}$ C in a 5%  $\text{CO}_2$  atmosphere.

Green live-cell membrane fluorescent dye DiO, red live-cell membrane fluorescent dye DiI, and blue live-cell nucleus fluorescent dye Hoechst 33342 were

purchased from Beyotime Biotechnology Co., Ltd. (Beijing, China). Agar was obtained from Beijing Dingguo Changsheng Biotechnology Co., Ltd. (Beijing, China). Matrigel (Cat# 356234) was acquired from Corning (USA). Whatman® lens cleaning tissue #105 was obtained from GE Healthcare Life Sciences (USA). All other chemicals were ordered from Aladdin Reagent Co., Ltd. (Shanghai, China) unless stated otherwise. All solutions were prepared with deionized water produced by a PURELAB flex system (ELGA, High Wycombe, UK).

## 2.2 Preparation of paper hybrid scaffolds

The agar/paper scaffolds were prepared according to our recent study (Xie et al., 2023). In brief, lens paper was cut into rectangles at a size of 1 cm×1 cm and sterilized by ultraviolet radiation for 1 h. Meanwhile, 1% (mass fraction) agar solution was sterilized by autoclaving. Then, the dip-coating method was applied to prepare agar/paper hybrid scaffolds. In the same way, the Matrigel/paper hybrid scaffolds were prepared by adding 10  $\mu$ L cold Matrigel (final concentration: 3 mg/mL in complete DMEM) to each piece of lens paper. After 5 min at room temperature, the superfluous Matrigel on the upper surface of lens paper was scraped carefully, and the remaining Matrigel was filled in the fibrous structure of lens paper.

## 2.3 Characterization of paper hybrid scaffolds

The agar/paper and Matrigel/paper hybrid scaffolds were imaged by a stereomicroscope (SZX2-ILLT, Olympus, Japan) for morphological characterization. Next, they were imaged by an inverted light microscope (TS100-F, Nikon, Japan) to observe the side view morphology.

## 2.4 Assembly and disassembly of the multilayer paper hybrid scaffold device

As shown in Fig. 1b, the multilayer paper-based device was composed of two polymethyl methacrylate (PMMA) plates: one with eight 8 mm-diameter holes and another without holes. The device housed a stack of three paper layers: the top and middle layers are Matrigel/paper, and the bottom layer is agar/paper. This paper stack was clamped between the two PMMA plates and secured at the corners with four screws. For disassembly after the cell culture experiments, the screws were removed to separate the paper layers,

which were individually placed in cell culture well plates for further analysis.

## 2.5 Nutrition transport test of the multilayer paper hybrid scaffold device

### 2.5.1 Solution absorption test

To evaluate the nutrient absorption capability of the hybrid scaffolds, 40  $\mu$ L of red food dye solution was applied to both the agar/paper and the Matrigel/paper samples, in order to simulate the absorption of cell culture medium nutrients. The samples were then examined under a stereomicroscope to assess their solution absorption efficiency.

### 2.5.2 Glucose transport test of the Matrigel/paper

To evaluate glucose transportation between the multilayer paper substrates, a gravity-driven glucose diffusion device was constructed, comprising eight top compartments and eight bottom compartments (Fig. 2). A glucose solution with a concentration of 16.8 mmol/L was consistently used in all experiments. Specifically, the glucose solution was placed in the top compartments, while pure water was placed in the bottom compartments. The one-layered or two-layered Matrigel/paper was positioned between the two compartments, followed by incubating the device at 37 °C. The glucose concentration in the top and bottom compartments was then measured using a glucometer (Sinocare, China) at different time points.

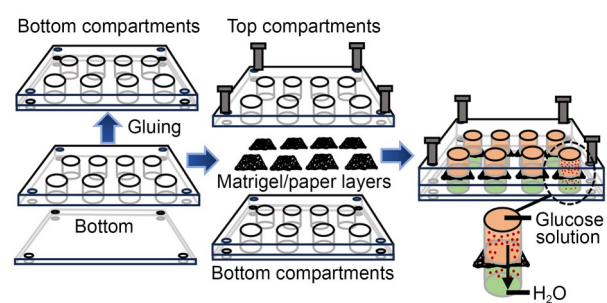


Fig. 2 Detection of glucose concentration in the upper and bottom compartments.

## 2.6 Cell co-culture in the multilayer paper hybrid scaffold device

### 2.6.1 Formation of DU145 spheroids on agar/paper

Sterilized agar/paper samples were placed into wells of a 48-well cell culture plate, followed by the

addition of 250  $\mu\text{L}$  of DU145 cell suspension ( $8.0 \times 10^5$  cells/mL). The plates were incubated at a cell incubator (37 °C and 5%  $\text{CO}_2$ ) for 24 h.

#### 2.6.2 Formation of endothelium layer on Matrigel/paper

Sterilized Matrigel/paper samples were placed into wells of a 48-well plate, followed by the addition of 250  $\mu\text{L}$  of HUVEC suspension ( $16.0 \times 10^5$  cells/mL). The plates were incubated in a cell incubator (37 °C and 5%  $\text{CO}_2$ ) for 24 h.

#### 2.6.3 Cell survival test in the device

In one group, three paper hybrid scaffolds with DU145 spheroids were assembled with PMMA clamps. In another group, one agar/paper sheet with DU145 spheroids and two Matrigel/paper sheets without cells were assembled with PMMA clamps. The two groups were cultured for 48 h, then the devices were disassembled, and viable cell numbers on each paper layer were assessed using the 3-(4,5-dimethylthiazol-2-yl)-2,5-diphenyltetrazolium bromide (MTT) proliferation assay.

#### 2.6.4 Measurement of DU145 spheroid volume after co-culture

One agar/paper sheet with DiI-stained DU145 spheroids, one Matrigel/paper sheet without cells, and one Matrigel/paper sheet with HUVECs were assembled with PMMA clamps. Then, NK-92 cell suspension ( $8.0 \times 10^5$  cells/mL) was added to each compartment for co-culture for two days. After disassembly, the length ( $L$ ) and width ( $W$ ) of DU145 spheroids were measured using ImageJ software, and volume ( $V$ ) was calculated using the formula:  $V=L \times W^2/2$  (Courau et al., 2019).

#### 2.6.5 Measurement of NK-92 cell-occupied and HUVEC-occupied areas after co-culture in the device

One agar/paper sheet with DU145 spheroids, one Matrigel/paper sheet without cells, and one Matrigel/paper sheet with DiI-stained HUVECs were assembled with PMMA clamps. Following the addition of DiO-labeled NK-92 cell suspension ( $8.0 \times 10^5$  cells/mL) and two days of co-culture, the device was disassembled. The cells on each paper layer were imaged from six randomly selected fields (TS100-F, Nikon), and then the areas occupied by DiO-stained NK-92 cells (green area) and the DiI-stained HUVECs (red area) were quantified by ImageJ software.

#### 2.6.6 Cells at each layer after co-culture counted by flow cytometry

In the DU145 group, one agar/paper sheet with DiI-stained DU145 spheroids, one blank Matrigel/paper sheet, and one Matrigel/paper sheet with HUVECs were stacked and placed in a single device. In the HUVEC group, one agar/paper sheet with DU145 spheroids, one blank Matrigel/paper sheet, and one Matrigel/paper sheet with DiI-stained HUVECs were stacked and placed in the device. Then, DiO-labeled NK-92 cells ( $8.0 \times 10^5$  cells/mL) were added into the two groups. After two days of co-culture, the devices and paper substrates were de-stacked. The cells at each layer were treated with trypsin digestion solutions (2.5 g/L) to prepare a single-cell suspension for flow cytometry analysis (NovoCyte™ 2060R, ACEA Biosciences, USA).

#### 2.6.7 Confocal microscopy of the tumor spheroids

One agar/paper sheet with Hoechst 33342-stained DU145 spheroids, one blank Matrigel/paper sheet, and one Matrigel/paper sheet with DiI-stained HUVECs were stacked and co-cultured with DiO-labeled NK-92 cells ( $8.0 \times 10^5$  cells/mL) for two days. Subsequently, the multilayer paper substrates were de-stacked, and tumor spheroids were collected by pipetting. The collected spheroids were resuspended in DMEM and imaged at different Z-axis planes using a confocal microscope (LSM 800, Zeiss, Germany).

### 2.7 Statistical analysis

All data were expressed as mean  $\pm$  standard deviation (SD). The results were analyzed by Student's *t*-test using GraphPad Prism software (Boston, MA, USA). *P* values less than 0.05 were considered statistically significant.

## 3 Results and discussion

### 3.1 Establishment of multilayer paper co-culture system by dip-coating the agar/Matrigel in the lens paper

In our recent report (Xie et al., 2023), we have established the suitability of agar/paper as a substrate for tumor spheroid formation. The compatibility of agar/paper with direct observation under a light microscope and the ease of collection of tumor spheroids

make it an ideal choice for developing a multilayer paper co-culture system. In this study, we utilized Matrigel, a well-known promoter of cell growth, as an ECM to facilitate cell invasion and combined it with paper to create Matrigel/paper, also referred to as gel in paper, which served as the middle invasion layer for the spheroid. The top layer of the co-culture system consisted of HUVECs seeded on Matrigel/paper (Fig. 3a). The visual representations in Fig. 3b demonstrate that the thicknesses of agar/paper and Matrigel/paper remained between 40–60 μm. The stacked three-layer paper samples had an average thickness of approximately 141.75 μm, providing an appropriate thickness to evaluate the invasion and migration potential of NK-92 cells in attacking the tumor spheroids located on the bottom layers. Furthermore, we conducted experiments involving various shapes, such as spreading, folding, and rolling the agar/paper and Matrigel/paper combinations, as detailed in Fig. 3c. The images demonstrate that agar/paper and Matrigel/paper both display favorable mechanical properties, thereby facilitating the successful implementation of the multilayer paper co-culture system.

### 3.2 Nutrition transport for cell growth through the Matrigel/paper hybrid scaffold

For the effective growth of cells within paper scaffolds, it is crucial to ensure their ability to absorb nutrients from the culture medium. We assessed this by staining Matrigel/paper and agar/paper hybrids with red dye and compared them with pure lens paper. As shown in Fig. 4a, the hybrid specimens absorbed dye in both their fibers and the internal gel matrix, unlike the lens paper that only absorbed dye into its fibers,

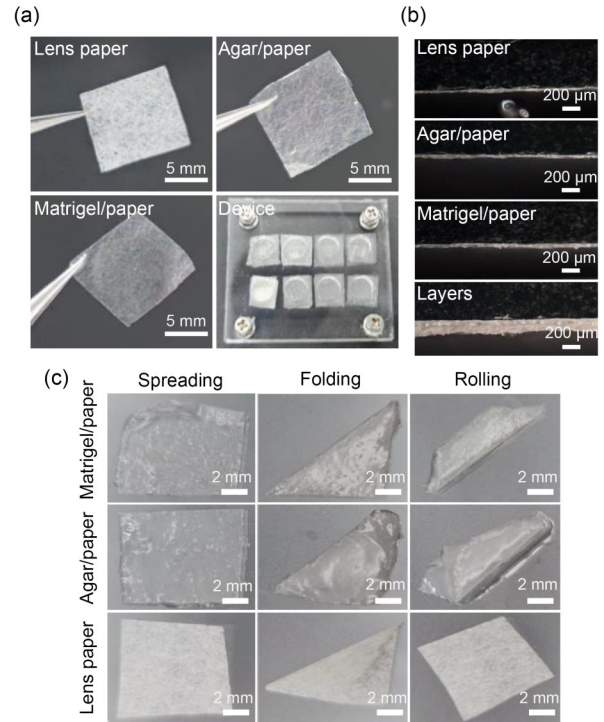


**Fig. 3** Characterization of the hybrid scaffolds. (a) Images of paper hybrid scaffolds and the multilayer paper co-culture device. (b) Side-view images of the paper hybrid scaffolds and multilayer paper. (c) Spreading, folding, and rolling of paper specimens.

indicating their superior nutrient absorption ability that is crucial for cell growth.

The transport of nutrients through the multilayer paper scaffolds was found to be a critical factor influencing cell growth, with the number of paper layers playing a significant role in this process (Simon et al., 2016; Boyce et al., 2017). Given the importance of glucose, a key nutrient in cell culture medium, in cell

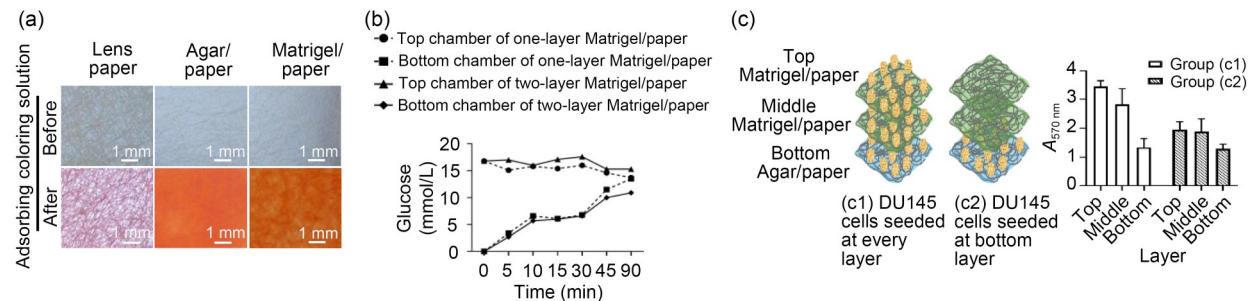


**Fig. 4** Nutrient diffusion and oxygen gradient between the multiple layers. (a) Images of the paper hybrid scaffolds before and after adsorbing coloring solution. (b) Glucose concentration at the top and bottom compartments from 0 to 90 min. (c) Left panel: schematic drawing of multilayer paper for the cell culture; group (c1) cells were seeded at each layer and group (c2) cells were seeded at the bottom layer. Right panel: living cells in the multilayer paper-based device measured by 3-(4,5-dimethylthiazol-2-yl)-2,5-diphenyltetrazolium bromide (MTT) assay. The absorbance values at 570 nm ( $A_{570 \text{ nm}}$ ) are expressed as mean±standard deviation (SD),  $n=3$ .

culture experiments, we investigated the transport of glucose as a nutrient example by a diffusion device at a temperature of 37 °C for 90 min. The setup, illustrated in Fig. 2, allowed the observation of glucose molecules moving from a glucose-rich top compartment to a bottom compartment filled with pure water. The results indicated an initial rise in glucose levels in the bottom compartment to about 6 mmol/L within 10 min for both the single- and double-layered scaffolds (Fig. 4b). The levels remained stable until 30 min into the experiment, and then increased significantly up to 90 min, reaching 13.5 and 10.9 mmol/L for the single- and double-layered scaffolds, respectively. The glucose concentration in the top compartment slightly decreased over 90 min. This demonstrates the efficiency of Matrigel/paper scaffolds in glucose transport, ensuring the provision of essential nutrients for cell growth within this timeframe. Previous research has highlighted the effectiveness of using stacked paper to create a 3D environment that supports cell invasion and growth. These multilayer paper scaffolds feature the formation of an oxygen gradient, with higher oxygen levels at the top and lower levels at the bottom (Mosadegh et al., 2015; Kenney et al., 2016). The impact of this gradient on cell viability and migration was explored by examining the survival of DU145 cells across different layers in two setups: one with cells seeded on each layer (c1), and one with cells seeded only at the bottom layer (c2) (Fig. 4c). After 48 h of culture, the proliferating cells in each layer were quantified. The results depicted in Fig. 4c show a higher cell count in the top layer compared with the bottom layer in setup (c1). Moreover, in setup (c2), despite cells being seeded only at the bottom layer initially, we could observe cell migration to the middle and even the top layer. These suggest that the increased cell numbers in the middle and top layers were due to a combination of cell proliferation and migration from the bottom layer. From these findings, we inferred that cells in the top layer benefit from an adequate oxygen supply, while those in the bottom suffer from oxygen scarcity. Therefore, cells in the lower layers tend to migrate upwards, seeking microenvironments with more oxygen and nutrients.

### 3.3 Interaction of tumor cells and NK cells in the multilayer paper co-culture device

In order to investigate the migration of NK-92 cells within the multilayer scaffold, we established

a co-culture system featuring DU145 cancer cells, HUVEC endothelial cells, and NK-92 cells. The experiment started with the assembly of paper hybrid scaffolds and hydrophobic PMMA clamps to prevent medium leakage, ensuring that cell movement could only occur through the Matrigel/paper scaffold. Within the multilayer paper stacks, the tumor spheroids on the bottom agar/paper layer simulated solid tumors, with the middle Matrigel/paper acting as the ECM and the top layer simulating the endothelial barrier to immune cells. NK-92 cells, introduced to target the tumor spheroids, represented immune cells navigating through these barriers. The human immortalized prostatic cell line PNT1A served as the control for normal cells and was co-cultured with HUVECs and NK-92 cells. As shown in Fig. 5a, before stacking the multilayer paper for co-culturing, DU145 spheroids and PNT1A spheroids were grown on the bottom agar/paper layer.

After 48 h of co-culturing tumor cells, HUVECs, and NK-92 cells, the structure was dismantled for analysis. Microscopic examination revealed that DU145 spheroids persisted in both the bottom and middle layers, indicating their invasive potential (Fig. 5b). In contrast, PNT1A cells showed weaker invasion activity, mostly remaining in the bottom layers (Fig. 5b). The length ( $L$ ) and width ( $W$ ) of the spheroids at the bottom and middle layers were determined from the microscopic images using ImageJ software (Fig. 5c). For the DU145 spheroids, the volume was from  $229.58 \times 10^4 \mu\text{m}^3$  before co-culture, with a length/width of  $195.78 \mu\text{m}/135.58 \mu\text{m}$ , to  $115.37 \times 10^4 \mu\text{m}^3$  after co-culture at the middle layer, with a length/width of  $161.04 \mu\text{m}/104.52 \mu\text{m}$  (Figs. 5c and 5d). Meanwhile, for PNT1A cells, the volume of the spheroids changed from  $45.74 \times 10^4 \mu\text{m}^3$  before co-culture, with a length/width of  $102.79 \mu\text{m}/89.73 \mu\text{m}$ , to  $44.51 \times 10^4 \mu\text{m}^3$  after co-culture at the middle layer, with a length/width of  $126.82 \mu\text{m}/79.45 \mu\text{m}$  (Figs. 5c and 5d).

Our next focus was on the interaction and distribution of DiO-labeled NK-92 cells within a three-layered scaffold, particularly their migration towards DU145 tumor spheroids. NK-92 cells navigated through the Matrigel/paper barriers, clustering around the spheroids in a targeted manner. This behavior was more pronounced in setups containing DU145 spheroids than in controls with PNT1A cells or no cells, indicating a specific attraction to tumor cells rather than a random distribution (Fig. 6a). Quantitative analysis

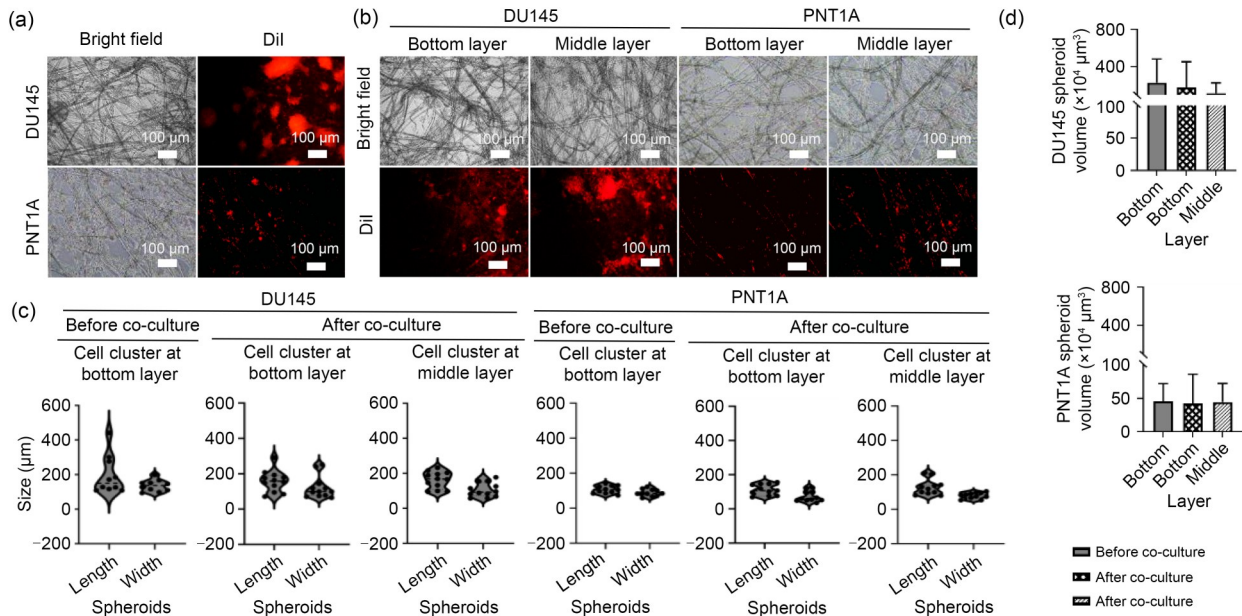


**Fig. 5** Characterization of DU145 and PNT1A spheroids in the multilayer paper. (a) Images of DiI-labeled DU145 and PNT1A cells on agar/paper after 24 h of seeding. (b) Images of DiI-labeled DU145 and PNT1A cells at the bottom and middle layers after 48 h of co-culture. (c) Lengths and widths of DU145 and PNT1A spheroids obtained by the measurement function of ImageJ. (d) Volumes of DU145 and PNT1A spheroids obtained by the particle analysis function of ImageJ. Volumes are expressed as mean±standard deviation (SD),  $n=10$ .

using ImageJ revealed significant differences in the distribution of NK-92 cells across the layers. In the DU145 group, the bottom layer had fewer NK-92 cells compared with the middle and top layers, with  $P$  values of 0.0439 and  $<0.0001$ , respectively (Fig. 6c). The invasion depth of approximately  $90 \mu\text{m}$  through the Matrigel/paper layers to the tumor cells was notable. However, the gathering of NK-92 cells at the middle and bottom layers of the PNT1A co-culture group was significantly less, as the presence of DU145 spheroids markedly increased the occupied area of bottom NK-92 cells by 195.26% over PNT1A and by 400.23% over no cells, with  $P$  values of 0.0008 and  $<0.0001$ , respectively (Fig. 6c).

Endothelial cells (ECs) are crucial for forming blood vessel walls and facilitating tumor angiogenesis, a key process in anti-tumor therapy (Liang et al., 2021). To characterize the interaction between tumor spheroids on the bottom agar/paper layer and HUVECs on the top Matrigel/paper layer, we quantified the invasion of HUVECs into neighboring layers (Fig. 6b). Notably, the area occupied by HUVECs in the bottom layer was significantly less than those in the middle and top layers, with  $P$  values of  $<0.0001$  (Fig. 6c), indicating that only a portion of HUVECs invaded the

tumor DU145 spheroid layer. In addition, the area of middle HUVECs in the DU145 group was significantly greater than those in the PNT1A and no cell groups, with  $P$  values of 0.0002 and  $<0.0001$ , respectively (Fig. 6c). In addition, the co-localization of HUVECs with DU145 spheroids on the bottom layer, highlighted by the intense DiI signal, suggested a targeted interaction. As indicated by the cell occupation area heat map shown in Fig. 6d, the results highlight the significant impact of tumor spheroids on the distribution and behavior of NK-92 cells and HUVECs, demonstrating the system's potential for studying tumor-immune-endothelial cell interactions within a structured 3D environment.

### 3.4 Formation of TINKs promoted by the multilayer paper co-culture system

The crucial role of TINKs in the battle against tumors has been highlighted by numerous studies (Burger et al., 2019). The reduced cytotoxicity of tumor-infiltrating NK-92 cells has been demonstrated to possibly occur due to the dysfunction of NK cells that are responsible for eliminating tumor cells (Russick et al., 2020). Furthermore, the reliance on cell attachment for the interaction between tumor spheroids and

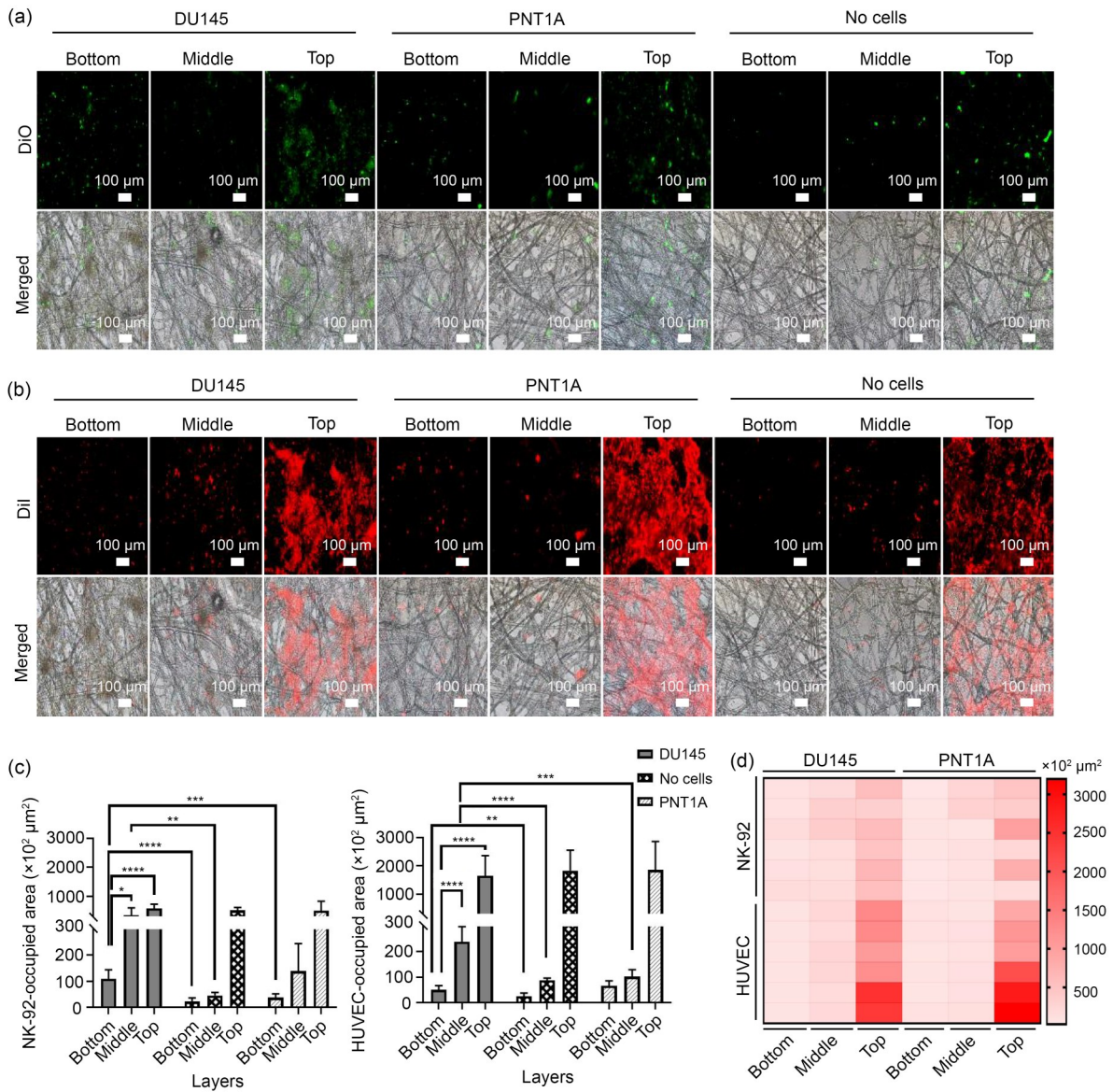


**Fig. 6** Behavioral characterization of human umbilical vein endothelial cells (HUVECs) and NK-92 cells in the multilayer paper stacks after 48 h of co-culture. (a) Images of DiO-labeled NK-92 cell distribution at each layer. (b) Images of DiI-labeled HUVEC distribution at each layer. (c) Areas occupied by NK-92 cells and HUVECs on each layer. Data are expressed as mean±standard deviation (SD),  $n=6$ . \* $P < 0.05$ , \*\* $P < 0.01$ , \*\*\* $P < 0.001$ , \*\*\*\* $P < 0.0001$ . (d) Heatmap of areas occupied by NK-92 cells and HUVECs on each layer.

NK-92 cells has been proven (Leung et al., 2020). Given these findings, our research aimed to utilize multilayer lens paper soaked in culture medium as a platform for TINK formation. After a 48-h co-culture period, tumor spheroids were extracted from both the bottom and middle layers for confocal microscope analysis to capture 3D and Z-axis images. As illustrated in Fig. 7a, cell clusters retrieved from the bottom and middle layers consisted of DU145 (blue), HUVEC (red), and NK-92 (green) cells. The co-localization of

these cells was indicated by orange spots, resulting from the blending of colors. Confocal microscopy revealed direct cell–cell contacts (Fig. 7b), including adherent and tight junctions, critical for the infiltration of NK-92 cells into tumor spheroids (Walter et al., 2023). The spheroids isolated from the different paper layers were further examined by the confocal Z-axis images to decipher the distribution of NK-92 cells within the spheroids (Fig. 7c). Specifically, at 4 μm intervals along the Z-axis, we observed NK-92 cells both

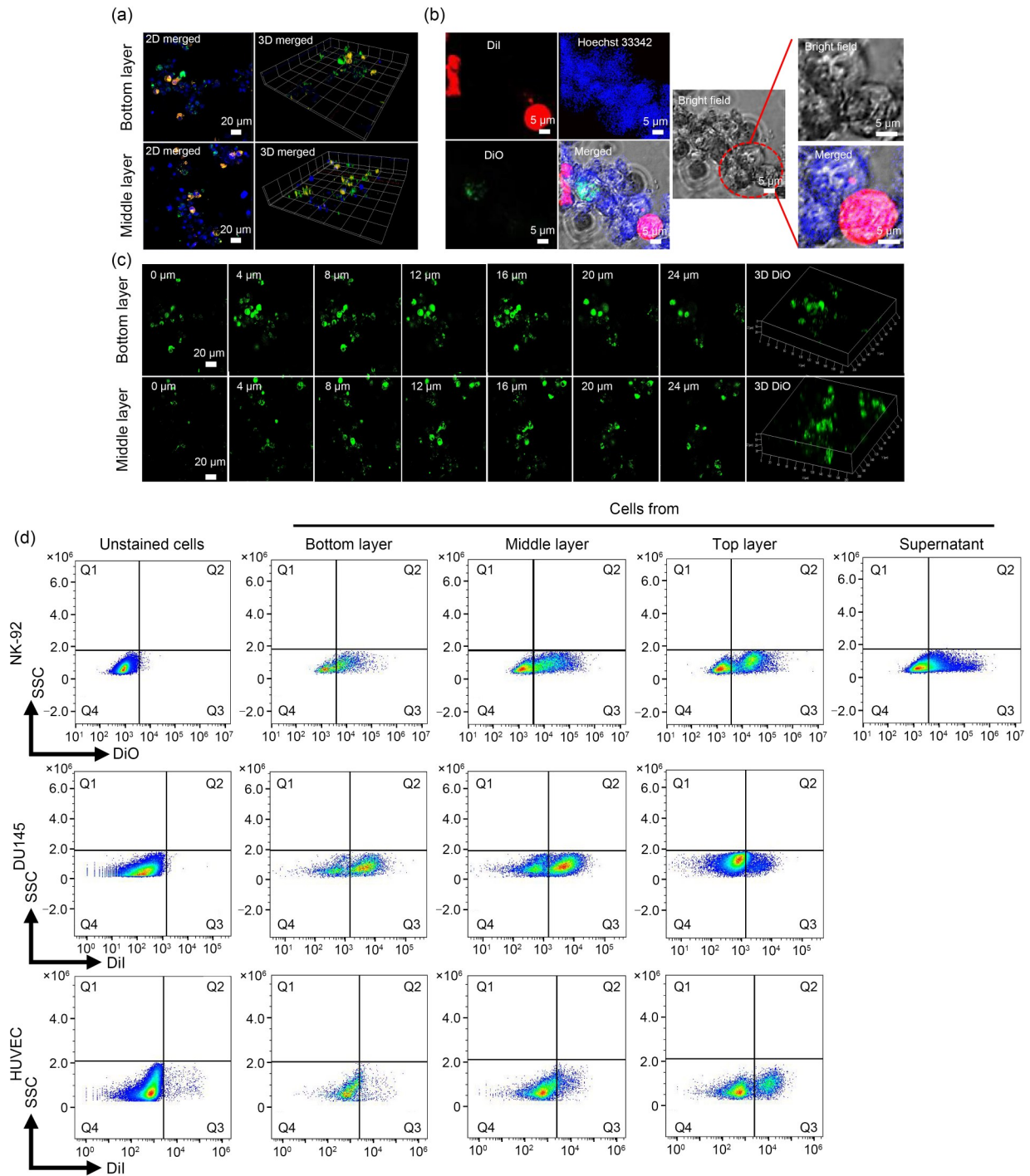


**Fig. 7** Characterization of tumor-infiltrating natural killer cells (TINKs) within tumor spheroids. (a) Confocal images of the collected tumor spheroids, with blue color denoting DU145, red color denoting human umbilical vein endothelial cells (HUVECs), and green color denoting NK-92. (b) Confocal images of spheroids isolated from the co-culture device. (c) Images of NK-92 cells at different Z-axis depths. (d) Flow cytometry counts of cells at each layer after co-culture of DU145, HUVEC, and NK-92 at the multilayer paper stack. SSC: side scatter.

on the outer surface and infiltrating the interior of spheroids. For example, NK-92 cells occupied areas of  $9.05 \times 10^2$  and  $10.32 \times 10^2 \mu\text{m}^2$  at 4 and 16  $\mu\text{m}$  depths,

respectively, in spheroids from the bottom layer. In addition, the multilayer paper-based device facilitated the quantification of cells at each layer after co-culture

to track the movement of cells. Flow cytometry was applied to quantify NK-92 cells, HUVECs, and DU145 tumor cells in the multilayer paper-based co-culture system. Fluorescent dye-labeled (DiO and DiI) cells could be observed at the Q3 area (Fig. 7d). Notably, DU145 cells showed a significant concentration in the middle layer, with fewer cells in the top layer. Specifically, cell counts in the middle layer exceeded those in the top and bottom layers (12 801 vs. 4129 vs. 4716), indicating a propensity for DU145 cells to localize predominantly in the middle layer. NK-92 cells were more abundant in the top layer compared with the middle and bottom layers (7900 vs. 5828 vs. 1878), while HUVEC counts decreased from top to bottom (3336 vs. 1093 vs. 465). The results indicate that the co-culture system utilizing multilayer paper facilitated the migration of NK-92 cells and the formation of TINKs. Our heterogenous multilayer paper co-culture platform not only enables the analysis of NK-92 cell infiltration but also provides valuable insights into cell attachment dynamics and the role of TINKs in tumor development. Further research in this area is expected to contribute to advancements in tumor immunotherapy and ultimately enhance patient outcomes.

#### 4 Conclusions

In this work, we developed a heterogeneous multilayer paper-based co-culture model of immune and tumor cells, utilizing agar/paper and Matrigel/paper hybrid scaffolds, to analyze nutrient transport, cell proliferation, and movement between the liquid culture media and tumor spheroids. The results prove that our device allows glucose transport to maintain cell viability and function. After a 48-h co-culture period, the migration of DU145 cells, NK-92 cells, and HUVECs was quantified using ImageJ and flow cytometry, which indicated that the multilayer paper supported cell growth and migration. The infiltration of NK-92 cells at different Z-axis depths within the tumor spheroids was probed using a confocal microscope, providing valuable insights into the behavior of immune cells within a tumor microenvironment. In summary, the proposed device successfully established a model of NKs traveling across the endothelium layer to form TINKs, which holds great promise for further investigations of the interaction dynamics of immune cells and cancer cells.

#### Data availability statement

The data in the current study are available from the corresponding authors upon reasonable request.

#### Acknowledgments

This work was supported by the National Natural Science Foundation of China (No. 32171401), the Natural Science Foundation of Chongqing (Nos. CSTB2022NSCQ-MSX0808 and cstc2021jcyj-bsh0239), and the Innovation Platform for Academicians of Hainan Province (No. YSPTZX202126), China.

#### Author contributions

Yuanyuan XIE: conceptualization, methodology, data curation, formal analysis, and writing – original draft. Xiaoyan YANG: methodology, investigation, and data curation. Rong PAN: methodology and data curation. Lixiao GAO: methodology and writing – review & editing. Ling YU: conceptualization, project administration, supervision, funding acquisition, and writing – review & editing. All authors have read and approved the final version of the manuscript, and therefore, have full access to all the data in the study and take responsibility for the integrity and security of the data.

#### Compliance with ethics guidelines

Yuanyuan XIE, Xiaoyan YANG, Rong PAN, Lixiao GAO, and Ling YU declare that they have no conflict of interests.

This article does not contain any studies with human or animal subjects performed by any of the authors.

#### References

- Agarwal T, Borrelli MR, Makvandi P, et al., 2020. Paper-based cell culture: paving the pathway for liver tissue model development on a cellulose paper chip. *ACS Appl Bio Mater*, 3(7):3956-3974. <https://doi.org/10.1021/acsabm.0c00558>
- Boyce MW, LaBonia GJ, Hummon AB, et al., 2017. Assessing chemotherapeutic effectiveness using a paper-based tumor model. *Analyst*, 142(15):2819-2827. <https://doi.org/10.1039/c7an00806f>
- Burger MC, Zhang CC, Harter PN, et al., 2019. CAR-engineered NK cells for the treatment of glioblastoma: turning innate effectors into precision tools for cancer immunotherapy. *Front Immunol*, 10:2683. <https://doi.org/10.3389/fimmu.2019.02683>
- Burster T, Gärtner F, Bulach C, et al., 2021. Regulation of MHC I molecules in glioblastoma cells and the sensitizing of NK cells. *Pharmaceuticals (Basel)*, 14(3):236. <https://doi.org/10.3390/ph14030236>
- Choi Y, Phan B, Tanaka M, et al., 2020. Methods and applications of biomolecular surface coatings on individual cells. *ACS Appl Bio Mater*, 3(10):6556-6570. <https://doi.org/10.1021/acsabm.0c00867>
- Courau T, Bonnereau J, Chicoteau J, et al., 2019. Cocultures of human colorectal tumor spheroids with immune cells

- reveal the therapeutic potential of MICA/B and NKG2A targeting for cancer treatment. *J Immunother Cancer*, 7(1):74.  
<https://doi.org/10.1186/s40425-019-0553-9>
- de Andrade LF, Lu YH, Luoma A, et al., 2019. Discovery of specialized NK cell populations infiltrating human melanoma metastases. *JCI Insight*, 4(23):e133103.  
<https://doi.org/10.1172/jci.insight.133103>
- Fontana F, Raimondi M, Marzagalli M, et al., 2020. Three-dimensional cell cultures as an in vitro tool for prostate cancer modeling and drug discovery. *Int J Mol Sci*, 21(18):6806.  
<https://doi.org/10.3390/ijms21186806>
- Fu JJ, Lv XH, Wang LX, et al., 2021. Cutting and bonding Parafilm® to fast prototyping flexible hanging drop chips for 3D spheroid cultures. *Cell Mol Bioeng*, 14(2):187-199.  
<https://doi.org/10.1007/s12195-020-00660-x>
- Gaitán-Salvatella I, López-Villegas EO, González-Alva P, et al., 2021. Case report: formation of 3D osteoblast spheroid under magnetic levitation for bone tissue engineering. *Front Mol Biosci*, 8:672518.  
<https://doi.org/10.3389/fmolb.2021.672518>
- Guo WJ, Chen ZJQ, Feng ZT, et al., 2022. Fabrication of concave microwells and their applications in micro-tissue engineering: a review. *Micromachines (Basel)*, 13(9):1555.  
<https://doi.org/10.3390/mi13091555>
- Kennedy RM, Boyce MW, Truong AS, et al., 2016. Real-time imaging of cancer cell chemotaxis in paper-based scaffolds. *Analyst*, 141(2):661-668.  
<https://doi.org/10.1039/c5an01787d>
- Larson TS, Glish GL, Lockett MR, 2021. Spatially resolved quantification of drug metabolism and efficacy in 3D paper-based tumor mimics. *Anal Chim Acta*, 1186:339091.  
<https://doi.org/10.1016/j.aca.2021.339091>
- Leung EYL, Ennis DP, Kennedy PR, et al., 2020. NK cells augment oncolytic adenovirus cytotoxicity in ovarian cancer. *Mol Ther Oncolytics*, 16:289-301.  
<https://doi.org/10.1016/j.omto.2020.02.001>
- Liang J, Wang SQ, Zhang GW, et al., 2021. A new antitumor direction: tumor-specific endothelial cells. *Front Oncol*, 11:756334.  
<https://doi.org/10.3389/fonc.2021.756334>
- Lin DG, Chen X, Lin Z, et al., 2021. Paper-supported co-culture system for dynamic investigations of the lung-tropic migration of breast cancer cells. *Biomed Mater*, 16(2):025028.  
<https://doi.org/10.1088/1748-605X/abc28c>
- Łuczynańska E, Anioł J, 2013. Neoangiogenesis in prostate cancer. *Contemp Oncol*, 17(3):229-233.  
<https://doi.org/10.5114/wo.2013.35272>
- Mosadegh B, Lockett MR, Minn KT, et al., 2015. A paper-based invasion assay: assessing chemotaxis of cancer cells in gradients of oxygen. *Biomaterials*, 52:262-271.  
<https://doi.org/10.1016/j.biomaterials.2015.02.012>
- Pan R, Yang XY, Ning K, et al., 2023a. Recapitulating the drifting and fusion of two-generation spheroids on concave agarose microwells. *Int J Mol Sci*, 24(15):11967.  
<https://doi.org/10.3390/ijms241511967>
- Pan R, Yang XY, Wu SM, et al., 2023b. Using pipette tips to readily generate spheroids comprising single or multiple cell types. *J Zhejiang Univ-Sci A (Appl Phys & Eng)*, 24(10):875-885.  
<https://doi.org/10.1631/jzus.A22D0235>
- Romo-Herrera JM, Juárez-Moreno K, Guerrini L, et al., 2021. Paper-based plasmonic substrates as surface-enhanced Raman scattering spectroscopy platforms for cell culture applications. *Mater Today Bio*, 11:100125.  
<https://doi.org/10.1016/j.mtbio.2021.100125>
- Russick J, Torset C, Hemery E, et al., 2020. NK cells in the tumor microenvironment: prognostic and theranostic impact. Recent advances and trends. *Semin Immunol*, 48:101407.  
<https://doi.org/10.1016/j.smim.2020.101407>
- Sang SB, Cheng R, Cao YY, et al., 2022. Biocompatible chitosan/polyethylene glycol/multi-walled carbon nanotube composite scaffolds for neural tissue engineering. *J Zhejiang Univ-Sci B (Biomed & Biotechnol)*, 23(1):58-73.  
<https://doi.org/10.1631/jzus.B2100155>
- Simon KA, Mosadegh B, Minn KT, et al., 2016. Metabolic response of lung cancer cells to radiation in a paper-based 3D cell culture system. *Biomaterials*, 95:47-59.  
<https://doi.org/10.1016/j.biomaterials.2016.03.002>
- Varudkar N, Oyer JL, Copik A, et al., 2021. Oncolytic parainfluenza virus combines with NK cells to mediate killing of infected and non-infected lung cancer cells within 3D spheroids: role of type I and type III interferon signaling. *J Immunother Cancer*, 9(6):e002373.  
<https://doi.org/10.1136/jitc-2021-002373>
- Walter K, Bourquin J, Amiri A, et al., 2023. Probing local lateral forces of focal adhesions and cell-cell junctions of living cells by torsional force spectroscopy. *Soft Matter*, 19(25):4772-4779.  
<https://doi.org/10.1039/d2sm01685k>
- Wu SM, Chen F, Yang XY, et al., 2023. Probing the interaction between metastatic breast cancer cells and osteoblasts in a thread-based breast-bone co-culture device. *Lab Chip*, 23(12):2838-2853.  
<https://doi.org/10.1039/d3lc00106g>
- Xie YY, Pan R, Wu SM, et al., 2023. Cell repelling agar@paper interface assisted probing of the tumor spheroids infiltrating natural killer cells. *Biomater Adv*, 153:213507.  
<https://doi.org/10.1016/j.bioadv.2023.213507>
- Zhao DK, Xu HQ, Yin J, et al., 2022. Inkjet 3D bioprinting for tissue engineering and pharmaceuticals. *J Zhejiang Univ-Sci A (Appl Phys & Eng)*, 23(12):955-973.  
<https://doi.org/10.1631/jzus.A2200569>